South African Journal of Chemical Engineering 45 (2023) 100–110

Contents lists available at ScienceDirect

South African Journal of Chemical Engineering

journal homepage: www.elsevier.com/locate/sajce

Optimization of the separation conditions of antioxidant peptides from red tilapia (*Oreochromis spp.*) viscera on cross-flow filtration ceramic membranes.

Lorena Arias, Claudia P. Sánchez-Henao, José E. Zapata *

Grupo de Nutrición y Tecnología de Alimentos, Universidad de Antioquia, calle 70 No. 52-21, Medellín, Colombia

ARTICLE INFO

Keywords:
Bioactive peptides
Enzymatic hydrolysis
Ultrafiltration
Design experiment
Central composite factorial design

SUMMARY

The enzymatic hydrolysate of red tilapia (*Oreochromis spp.*) viscera was fractionated by means of ceramic tubular membranes with a molecular weight of 3 kDa. For this purpose, a cross-flow filtration system operating with a positive displacement pump was designed, while in order to optimize the process, response surface methodology was used to evaluate the effect of pH, transmembrane pressure (TMP) and feed flow rate on volume reduction factor (VRF), fouling resistances and transmission of antioxidant peptides in the permeate.

According to the results obtained, the permeate flow yield was affected at acidic pH with a significant decrease due to membrane fouling. The polynomial models were optimized to find the best combination of response variables, indicating that the following are the optimum operating conditions: pH 8.39, 5 bar and 400 L/h. In addition, an increase in the antioxidant capacity of the permeate was obtained, enhancing the biological activity and indicating its possible use as a nutraceutical.

Abbreviations

AA	Amino acids
ABTS	Radical scavenging, μ-eqmol-trolox/g protein
ANOVA	Analysis of variance
CH	Centrifuged hydrolysate
DH	Degree of hydrolysis,%
E/S	Enzyme/substrate
FRAP	ferric reducing antioxidant power, μ-eqmol-trolox/g protein
J	flux (L/m2 h)
ORAC	Oxygen radical absorbance capacity, μ-eqmol-trolox /g protein
Rm	intrinsic membrane resistance (kPa m2 h/L)
Rr	Fouling resistance reversible, kPa m2 h/L
Rir	Fouling resistance irreversible, kPa m2 h/Lx
Rt	total membrane resistance (kPa m2 h/L)
T	Transmission of antioxidant peptides,%
TMP	Transmembrane pressure, bar
TRM	Treated raw material
Vo	feed volume (L)
Vr	retentate volume (L)
VRF	Volume reduction factor
μ	viscosity (Pa. s)

1. Introduction

Global fish production reached about 179 million metric tons in 2018. Of these, 156 million t were destined for human consumption. Red tilapia (*Oreochromis spp.*) is part of the main species produced in global aquaculture and represents 1.9% of finfish production (FAO, 2020). Traditionally, tilapia commercialization and industrialization processes for human consumption involve gill removal, evisceration, and scaling (Merino et al., 2013). This generaties large amounts of byproducts, which are generally discarded and cause numerous environmental problems (Villani et al., 2017). Fish viscera comprise 12% to 18% of the total weight of fish and are noted for containing a high percentage of water and lipids and for being an important source of protein (Villamil et al., 2017). The latter can be enzymatically hydrolyzed to obtain bioactive peptides (Halim et al., 2016; Montero-Barrantes, 2021), which are of great interest to the pharmaceutical and food industries (Sila and Bougatef 2016; Zheng et al., 2019). These play a very important role in health due to their antimicrobial, antithrombotic, antihypertensive, opioid, immunomodulatory, mineral-binding, and antioxidant action (Sanchez and Vazquez, 2017; Halim et al., 2016; Gianfranceschi et al.,

* Corresponding author.
E-mail addresses: slorena.arias@udea.edu.co (L. Arias), cpatricia.sanchez@udea.edu.co (C.P. Sánchez-Henao), edgar.zapata@udea.edu.co (J.E. Zapata).

https://doi.org/10.1016/j.sajce.2023.05.002
Received 11 August 2022; Received in revised form 7 January 2023; Accepted 5 May 2023
Available online 6 May 2023

2018).

Antioxidants can prevent the action of free radicals that can cause damage to biologically important molecules such as DNA, proteins, and phospholipids. A failure to prevent such damage could trigger the development of diseases such as atherosclerosis, arthritis, hypertension, diabetes, and cancer (Martínez-Medina et al., 2019). In a recent study, protein hydrolysates from red tilapia (*Orechoromis spp.*) viscera were fractionated with polymeric membranes with different pore size in Amicon ultra-15 units and shake cells by conventional or transverse ultrafiltration, finding higher antioxidant activity in low molecular weight peptides (< 3 kDa and <1 kDa) (Sepúlveda and Zapata, 2020; Gómez et al., 2019). Furthermore, it was determined that these fractions protected Caco-2 cells from H_2O_2-induced oxidative stress without affecting the viability of healthy cells nor modifying the stages of their cell cycle (Gómez et al., 2019). However, in this study, membranes in laboratory test tubes and devices with a size of the order of mL were used, which creates the need to search for conditions that allow this process to be pushed to a larger scale and the implementation of continuous production systems of these peptides.

Membrane separation technology is a nondestructive physicochemical technique in which the compounds in the permeate retain the biological activity they possessed in the feed (Nath et al., 2018; Castro-Muñoz et al., 2018), while it is cost-effective and environmentally friendly (Roslan et al., 2017). However, different aspects must be considered when selecting a membrane system for an industrial application. These include chemical, mechanical, and thermal resistance as well as flow recovery capacity and durability of the manufacturing material (Solís et al., 2017). In this sense, ceramic membranes outperform polymeric membranes, although the latter are more expensive (Abdullayev et al., 2019).

Filtration with ceramic membranes has been used for fractioning bioactive peptides of low molecular weight, obtained from different raw materials, including vegetable sources such as corn gluten meal (Liu et al., 2020) and wheat gluten (Liu et al., 2021). Also, food proteins derived from the fish industry, as the residual water generated during shrimp (Tonon et al., 2016) and salmon's head processing (Hanachi et al., 2022) has been used. They have also been applied to obtain peptides from fish by-products to study their nutritional quality in tuna muscle. (Saidi et al., 2014) and their sensorial and chemical properties in salmon and mackerel (Aspevik et al., 2021).

An unavoidable phenomenon in membrane processes is fouling, which gradually reduces permeate flow and increases hydraulic resistance, therefore decreasing overall process productivity (Park et al., 2018). Proteins are one of the main compounds responsible for membrane fouling. Fundamentally, this is due to protein-protein and protein-membrane interaction forces (Wen-qiong et al., 2019), which are affected by different factors, including pH (Navarro-Lisboa et al., 2017).

In the present study, a cross-flow filtration system with ceramic membranes was implemented. In this system, the operating conditions were optimized for the separation of antioxidant peptides from enzymatic hydrolysates of red tilapia (*Oreochromis spp.*) viscera. The response surface methodology was chosen for this purpose and applied by means of a central composite factorial design to evaluate the effect of transmembrane pressure (TMP), feed flow rate (L/h) and pH on the response variables: fouling resistance, transmission of antioxidant peptides (T), and volume reduction factor (VRF).

2. Methodology

2.1. Raw material handling

The red tilapia (*Oreochromis spp.*) viscera were collected at the El Gaitero fish farm located in the municipality of Sopetrán - Colombia (South America) and transported to the research laboratory in styrofoam coolers with refrigerant gels to preserve the cold chain. The same day they were collected, the viscera were heated at 90 °C for 20 min. to inactivate the endogenous enzymes and favor fat separation. They were then allowed to cool and stored at −18 °C for 24 h. The next day, the fat layer was removed from the top and homogenized in a food processor (Quick'n Easy, Black&Decker, USA) (Gómez et al., 2019). This is referred to as treated raw material (TRM).

2.2. Viscera and hydrolysate characterization

Samples of fresh, defatted red tilapia viscera and the hydrolysate were analyzed in triplicate according to the official methods of analysis AOAC (1984): moisture determination, using a moisture balance with halogen lamp model MOC63 (Shimadzu, Japan). The analysis of protein content was made with the micro Kjendahl technique, using a DK 12 heating digester (Velp Scientifica, USA). The ethereal extract was determined according to the official solvent extraction method, using a Starfish (Radleys, United Kingdom) Soxhlet extractor with petroleum benzine as solvent. To determine the ash content, the samples were calcined at 550 °C in a muffle model D8 (Terrigen, Colombia).

2.3. Enzymatic hydrolysis of defatted viscera

Hydrolysis was carried out in a New Brunswick Bioflo & celligen 310 bioreactor (Eppendorf, Germany) with a working volume of 6 L. The TRM was added at protein concentration of 10 g/L and the pH was adjusted to 10 with NaOH 2N. Subsequently, the enzyme Alcalase 2.4 L® was added at an enzyme/substrate (E/S) ratio of 20% at 59.1 °C, maintaining an agitation of 51 rpm. The hydrolysis time was 3 h, according to the methodology described by Sepúlveda and Zapata (2020), after which the hydrolysate was heated at 90 °C for 15 min to inactivate Alcalase 2.4 L®. The hydrolysate was cooled and centrifuged at 8500 rpm for 10 min in a refrigerated centrifuge U-320R (Boeco, Germany), and finally the supernatant was collected and stored at −18 °C.

The reaction was monitored by means of the degree of hydrolysis (DH) (Eq. (1)), expressed as the ratio between the number of peptide bonds cleaved in hydrolysis (α) and the number of total peptide bonds in the native protein, per unit weight (h_t). For this case, a h_t of 8.22 Eqv/kg was taken (Gómez et al., 2019).

$$\boldsymbol{DH} = \frac{BN_B}{M_P}\ \frac{1}{\alpha}\ \frac{1}{h_t} * 100 \tag{1}$$

$$\boldsymbol{\alpha} = \frac{10^{pH-pK}}{1 + 10^{pH-pK}} \tag{2}$$

$$\boldsymbol{pk} = 7,8 + \frac{298 - T}{298 * T} * 2400 \tag{3}$$

Where B is the Volume consumed of base in L, Nb = Normality of base (Eqv/L), Mp is Mass of protein in kg, and α is the degree of dissociation of α-NH groups$_2$ released in the reaction. This depends on the pK, which in turn is associated with temperature (Gómez et al., 2013).

2.4. cross-flow filtration system

The centrifuged hydrolysate (HC) was fractionated in a filtration system with INSIDE CéRAM™ (TAMI industries, France) ceramic tubular membranes 25 cm long, and consisted of a support made of a mixture of aluminum/titanium/zirconium oxides with an active layer of titanium oxide, furthermore, in order to have a better use of the membranes, the manufacturer recommends using a tangential velocity between 2–4,5 m/s (equivalent to 202–454,5 L/h). A 3 kDa cutoff molecular weight membrane was used because peptides below this cutoff point have been effective in eliminating free radicals, as is the case for hydrolyzed Corvina (*Pseudosciaena crocea*) muscle (Chi et al., 2015), tuna (*Thunnus albacores*) viscera (Pezeshk et al., 2019), muscle from the fish *Nemipterus hexodon* (Nalinanon et al., 2011) and byproducts from

gilt-head bream (*Sparus aurata*) and European bass (*Dicentrarchus labrax*) (Valcárcel et al., 2020). In addition, the cross-filtration was carried out at ambient temperature (25 °C), and was evaluated in membranes of 1, 15 y 50 kDa (results not shown), which resulted in poorer results than the obtained when using the 3 kDa membrane.

The system designed operated with a positive displacement rotary vane pump Procon Series 3 (Standex, USA), coupled to a ¾ HP Marathon motor (ABSA, Mexico), which allows the operator to work with a maximum pressure of 15 bar and 500 L/h, a frequency converter (ACS310 from ABB, Switzerland), a valve, two manometers, and a magnetic flow meter (2551 +GF+, USA), according to the scheme shown in Fig. 1.

2.5. Filtration process

The new 3 kDa membrane was conditioned before each HC filtration experiment. This activation procedure was initially based on hydration process involving the recirculation of distilled water with a feed flow rate of 400 L/h, 50 °C and TMP 1.5 bar for a time of 1.5 h. Finally, the same cleaning treatment that is used on the membrane was applied after the filtration cycle (Urbanowska and Kabsch-Korbutowicz, 2019).

In each test, the initial and final resistance of the membrane was determined to establish the efficiency of chemical cleaning. For this purpose, distilled water was recirculated through the retention channel at a rate of 400 L/h, taking different TMP data versus permeate flow. Plotting these two variables produces a slope representing the corresponding resistance (Lyu et al., 2019).

Membrane cleaning was performed in three stages: one consisted of a rinse with distilled water after finishing the HC filtration, then chemical cleaning was performed with a 20 g/L solution of NaOH for one hour at a TMP of 1.5 bar, and the membrane was finally rinsed with distilled water until a neutral pH was reached (Espejo-Carpio et al., 2015).

2.6. Filtration process variables

2.6.1. Antioxidant activity

Both HC and permeate were evaluated for antioxidant activity. This analysis was performed in 96-cup microplates in a Varioskan LUX device (Thermo scientific, USA). By means of in vitro techniques such as ferric reducing antioxidant power (FRAP), ABTS radical scavenging, both following the methodology of Vasconcelos et al. (2019) and oxygen radical absorbance capacity (ORAC) with the method described by Liu et al. (2018).

2.6.2. Peptide transmission (T)

The concentration of peptides in the feed and in the permeate is calculated. Transmission is defined as the ratio between the peptide concentration in the permeate Cp and the feed Ca. This is calculated based on Eq. (4). The peptide concentration is measured based on the antioxidant activities (ABTS, FRAP, and ORAC).

$$T(\%) = \frac{Cp}{Cr} * 100 \tag{4}$$

Where: Cp is the concentration of antioxidant peptides in the permeate and Cr is the concentration of antioxidant peptides in the retentate.

2.6.3. Volume reduction factor

It is the ratio between the feed volume (Vo) and the retentate volume (Vr). This parameter is important due to its relationship with process productivity. This was calculated based on Eq. (5).

$$VRF = \frac{V0}{Vr} = \frac{V0}{V0 - Vp} \tag{5}$$

Where Vp is the volume of permeate

2.6.4. Fouling resistance

Fouling resistance is reversible (Rr) and irreversible (Rir). The former refers to fouling that can be removed by rinsing with water, whereas the latter is the fouling both on the surface and inside the membrane pores Luján-Facundo et al., 2017). Both resistances were calculated based on Eqs. (6) and ((7). This series resistance model involves the hydraulic resistances on the evolution of permeate flow (J) over time, which are related according to Darcy's Law (Eq. (6)) (Li et al., 2018).

$$J = \frac{TMP}{\mu Rt} = \frac{TMP}{\mu(Rm + Rf)} \tag{6}$$

$$Rf = Rr + Rir \tag{7}$$

Where J is the flux (L/m^2 h), TMP is the applied transmembrane pressure (bar), μ is the water viscosity (Pa. s), and Rt and Rm are the total and intrinsic membrane resistances (kPa m^2 h/L), respectively.

Rt was determined by measuring the resistance of the dirty membrane at the end of each filtration test with the working fluid.

2.7. Optimization of the operating conditions for cross-flow filtration

Initially, an experimental design was proposed to evaluate the effect

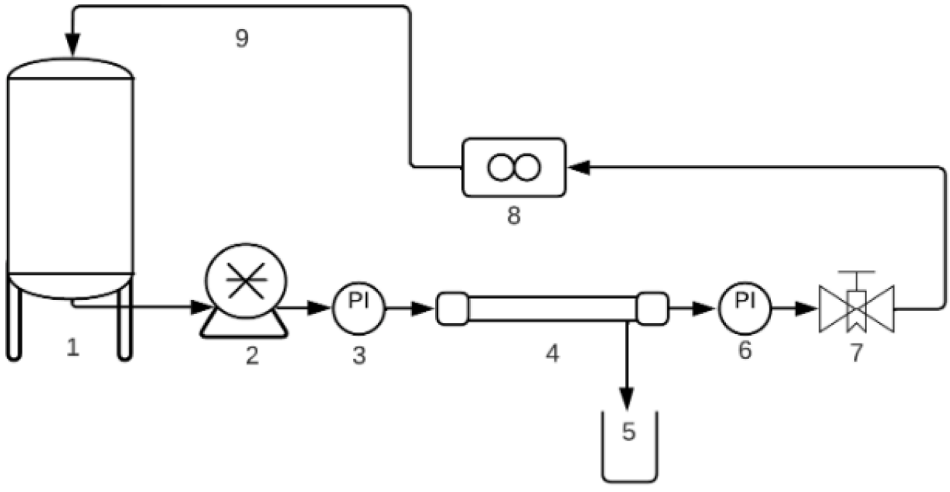

Fig. 1. Diagram of the cross-flow filtration system. 1. Feed tank; 2. Pump 3. Pressure gage; 4. Tubular membrane module; 5. Permeate vessel; 6. Pressure gage 7. valve; 8. Flowmeter; 9. Retentate.

Table 1
Central composite factorial design.

Run	pH	TMP (bar)	Feed flow rate (L/h)
1	2.76	3.5	425
2	7	3.5	390
3	10	2	450
4	11.24	3.5	425
5	7	5.6	425
6	7	3.5	425
7	7	3.5	425
8	7	1.38	425
9	7	3.5	425
10	7	3.5	425
11	7	3.5	425
12	10	5	400
13	4	5	450
14	4	2	400
15	7	3.5	460

Table 2
Physicochemical characterization of red tilapia (*Oreochromis spp.*) viscera.

Component	Viscera (%)	Defatted víscera (%)
Humedad	61.23 ± 1.36	86.10 ± 1.71
Proteína	4.07± 0.41	8.61 ± 0.88
Lípidos	34.02 ± 1.13	2.74 ± 0.76
Cenizas	0.84 ± 0.20	1.73 ± 0.28

of operating conditions on the main parameters of filtration, the Design Expert software (Stat-Ease Inc, USA) was used. Response surface methodology was applied using a central composite factorial design. A total of 15 experimental runs were carried out, considering three factors (two levels for each one) and four response variables (Table 1). The factors considered were TMP (2 - 5 bar), pH (4–10) and feed flow rate (400–450 L/h). The response variables were (T, VRF, R_r and R_{ir}). The analysis of the design was done by ANOVA, which allows obtaining a model representation for each response variable, as shown in Eq. (8):

$$Y = \beta_0 + \sum_{i=1}^{n} \beta_i X_i + \sum_{1 \le i \le j}^{n} \beta_{ij} X_i X_j + \varepsilon \quad (8)$$

Where: Y is the predicted response variable (T, VRF, Rr or R_{ir}), X_i are the uncoded values of the factors (TPM, pH, Feed flow rate), β_0 is a constant, β_i are the coefficients of the main effects for each factor, β_{ij} are the coefficients of the effect of the interactions, and ε is the error.

For each response Y (*i.e.,* T, VRF, Rr or R_{ir}), a statistical model was obtained, whose goodness of fit was assessed using the coefficients of correlation (R^2 the adjusted R^2), the lack of fit, and adequate precision (Adeq precision). The obtained models were used for optimization, and the optimal conditions found were validated against experimental runs by triplicate.

Additionally, retention coefficients were calculated according to Eq. (9) and a mass balance was performed to evaluate the possible loss of antioxidant activity or protein, respectively.

$$R(\%) = \left(1 - \frac{Cp}{Ca}\right) * 100 \quad (9)$$

Where: Cp is the concentration of antioxidant peptides in the permeate and Ca is the concentration of antioxidant peptides in the feed solution.

2.8. Amino acid analysis

The hydrolysate and freeze-dried fractions were subjected to acid hydrolysis using 6N HCl and 0.1% phenol at 110 °C for 18 h to release all amino acids (AA). The AA were determined and quantified by HPLC using a Dionex Ultimate 3000 device (Thermo Fisher Scientific, USA). In order to perform the analysis of AA, the samples were derivatized in situ using o-phthalaldehyde (OPA) for primary AA and 9-flourenylmethyl chloroformate (FMOC) for secondary AA. The device has an autosampler, a 5 μm analytical column, ZORBAX Eclipse AAA-C18, 4.6 × 75 mm (Agilent, USA) and gradient for the mobile phase; this is a mixture of water-methanol-acetonitrile (10:45:45) and 40 mM phosphate buffer (pH 7.8) (Cigić et al., 2008).

3. Results and discussion

3.1. Characterization of red tilapia (Oreochromis spp.) viscera

Pretreatment of the substrate is an important step in enzymatic hydrolysis as the fat content must be controlled. This is due to the fact that lipids found in red tilapia viscera at high concentrations act as inhibitors of the enzyme Alcalase 2.4 L® in the enzymatic protein hydrolysis reaction (Gomez et al., 019). In addition, the remaining lipids in the viscera are susceptible to oxidation, which can affect the commercial and nutritional value of the final product (Liu et al., 2014). According to the characterization performed (see Table 2), a 92% reduction in lipids and a 111% increase in proteins were achieved; these conditions favor the separation process.

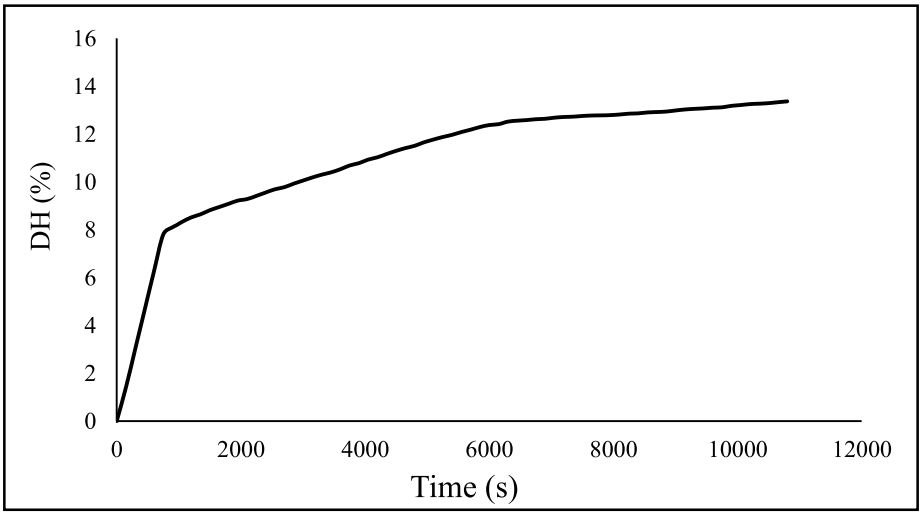

Fig. 2. Kinetics of the degree of hydrolysis of Alcalase 2.4 L® in red tilapia (*Oreochromis* spp.) viscera.

Table 3
Response variables of the central composite factorial experimental design.

Run	VRF	Rr (kPa*m^2*h/L)	Rir (kPa*m^2*h/L)	T ORAC (%)	T ABTS (%)	T FRAP (%)
1	1.072	16.180	19.951	77.7 ± 0.2	104.1.3 ± 4.5	107.9 ± 8.6
2	1.236	2.951	10.288	126.7 ± 5.3	104.1.5 ± 4.0	150.7 ± 5.1
3	1.140	5.993	7.429	106.2 ± 4.9	116.7 ± 1.6	141.9 ± 2.8
4	1.333	2.827	8.455	69.2 ± 2.0	101.1 ± 0.7	116.1 ± 1.5
5	1.592	1.039	10.402	117.6 ± 2.9	130.8 ± 1.7	125.3 ± 3.3
6	1.328	3.448	7.994	110.8 ± 3.0	123.8 ± 1.2	132.8 ± 1.4
7	1.280	4.264	7.340	114.2 ± 1.8	119.5 ± 1.2	127.7 ± 8.1
8	1.080	14.890	6.463	107.2 ± 5.3	132.2 ± 3.0	129.7 ± 5.1
9	1.345	3.489	7.507	115.8 ± 3.5	118.2 ± 1.7	123.4 ± 1.1
10	1.313	3.138	8.536	112.1 ± 1.3	122.5 ± 2.5	130.2 ± 0.7
11	1.309	4.210	8.719	119.8 ± 2.0	123.9 ± 1.6	129.4 ± 3.6
12	1.734	3.581	8.432	105.5 ± 3.2	118.1 ± 4.0	133.3 ± 1.6
13	1.113	4.118	33.846	79.6 ± 1.7	114.3 ± 4.7	115.7 ± 2.0
14	1.056	7.234	35.353	76.5 ± 2.7	99.5 ± 3.8	117.6 ± 7.4
15	1.352	2.704	7.136	104.4 ± 1.9	117.3 ± 3.5	128.3 ± 3.1

Table 4
ANOVA for the response variables of the Central Composite Factorial Design.

Source	P <0.05					
	VRF	Rr (kPa*m^2*h/L)	Rir (kPa*m^2*h/L)	T ORAC (%)	T ABTS (%)	T FRAP (%)
Model	< 0.0001	0.0026	0.0018	< 0.0001	0.0002	< 0.0001
A-pH	< 0.0001	0.0005	0.0613	0.0004	0.1375	< 0.0001
B- Feed flow rate	0.0109	0.8446	0.3846	0.0003	–	0.0006
C-TMP	< 0.0001	0.0009	0.2710	0.1854	0.0194	0.0799
AB	–	0.0249	–	–	–	–
AC	< 0.0001	–	–	0.0013	–	0.0014
BC	–	0.0053	0.0404	< 0.0001	–	–
A^2	0.0364	0.0282	0.0066	< 0.0001	< 0.0001	0.0062
B^2	0.0280	–	–	–	–	0.0024
C^2	–	0.0342	–	–	–	–
Lack of fit	0.1010	0.1453	0.0579	0.4061	0.1082	0.6756
R^2	0.99	0.92	0.85	0.98	0.92	0.95

3.2. Enzymatic hydrolysis of red tilapia (Oreochromis spp.) viscera proteins

The kinetic behavior of the enzymatic hydrolysis reaction of Alcalase 2.4 L® with red tilapia viscera reached a GH of 13.37 ± 0,04%, as shown in Fig. 2, indicating that the reaction product has potential as a bioactive hydrolysate, since it has been shown that values higher than 10% GH tend to generate hydrolysates with bioactive properties (Benítez et al., 2008). The bromatological characterization of this hydrolysate yielded 0.967 ± 0.005% protein, 1.236 ± 0.227% lipids, 0.209 ± 0.024% ash and 97.977 ± 0.151% moisture. High moisture content is due to the fact that it was prepared at 10 g/L protein. The low protein concentration points to the need to increase the concentration of the peptides of interest.

3.3. Effect of factors on cross-flow filtration responses of hydrolysates: Analysis of the experimental design

Table 3 shows the results of the response variables for each run of the experimental design. Table 4 shows the results of the statistical analysis of the design by ANOVA, which includes the coefficients of correlation (R^2 the adjusted R^2), the lack of fit, and adequate precision (Adeq precision). ANOVA indicated that all the analyzed factors affect significantly all the response variables, most of them in linear term, much of them in quadratic term and much interactions statistically significative between factors. Most of models have R^2 higher than 0.9, while the adjusted R^2 were higher than 0.8, let see that more than 80% of response variables can be explain from the factors, most case except to R_{ir}. For the Adeq Precision parameter, which measures the signal to noise ratio, a ratio greater than 4 is desirable. In all cases, this ratio is higher than 4, which indicates that these models can be used to navigate the design space. All models were significant at 95% confidence with lack of fit not significant for all response variables, so it can be stated that the obtained models are an adequate representation of the response variables.

From the ANOVA, models were defined Eqs. (10)-((15)) containing the significant terms (p<0.05) from which the figures of the response surfaces were constructed (Figs. 3-8) describing the graphical behavior of each response as a function of the factors, where the blue colors indicate the minimum values, the green colors indicate the mean values, and the red colors indicate the maximum values of the response variables.

$$\mathrm{VRF} = -6.296 - -(0.0433*\mathrm{pH}) + (0.0344*\mathrm{Feedflowrate}) - (0.156*\mathrm{TMP}) + (0.039*\mathrm{pH}*\mathrm{TMP}) - - \left(2.570\mathrm{E}-003*\mathrm{pH}^2\right) - (0.3855\mathrm{E}-005*\mathrm{Feedflowrate}^2) \quad (10)$$

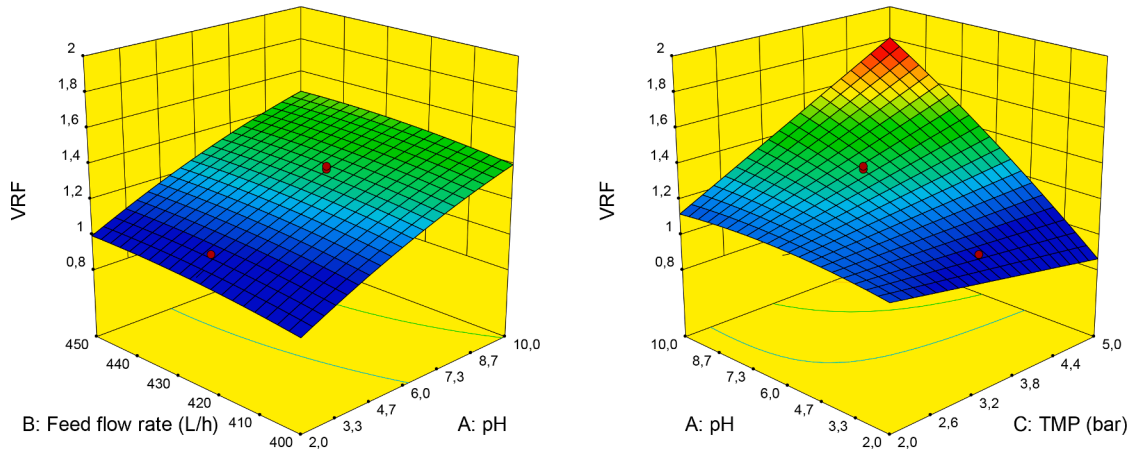

Fig. 3. Response surface for the parameter VRF as a function of pH, TMP and feed flow rate, predicted by Eq. (10).

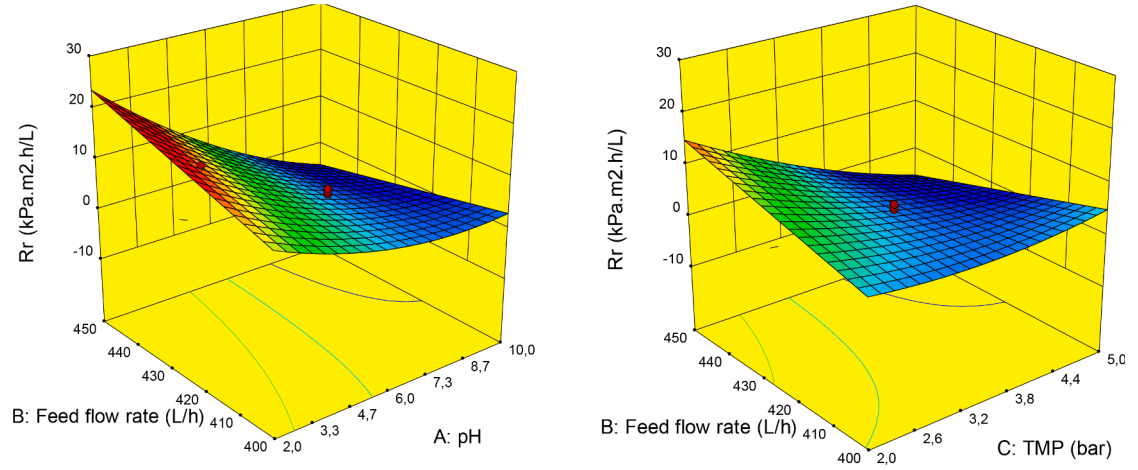

Fig. 4. Response surface for the parameter reversible resistance as a function of pH, TMP and feed flow rate, predicted by Eq. (11).

$$\mathrm{Rr} = -302.448 + (16.107*\mathrm{pH}) + (0.824*\mathrm{Feedflowrate}) + (50.153*\mathrm{TMP}) - (0.049*\mathrm{pH}*\mathrm{Feedflowrate}) - - (0.139*\mathrm{Feedflowrate}*\mathrm{TMP}) + (0.203*\mathrm{pH}^2) + (0.778*\mathrm{TMP}^2) \quad (11)$$

$$\mathrm{Ln(Rir)} = +23.805 - (0.620*\mathrm{pH}) - (0.0456*\mathrm{Feedflowrate}) - (5.042*\mathrm{TMP}) + (0.012*\mathrm{Feedflowrate}*\mathrm{TMP}) + (0.037*\mathrm{pH}^2) \quad (12)$$

$$\mathrm{TORAC} = -735.870 + (46.153*\mathrm{pH}) + (1.558*\mathrm{Feedflowrate}) + (264.538*\mathrm{TMP}) - (2.787*\mathrm{pH}*\mathrm{TMP}) - - (0.573*\mathrm{Feedflowrate}*\mathrm{TMP}) - - (2.878*\mathrm{pH}^2) \quad (13)$$

$$\mathrm{TABTS} = +54.317 + (15.860*\mathrm{pH}) + (2.765*\mathrm{TMP}) - (1.075*\mathrm{pH}^2) \quad (14)$$

$$\mathrm{TFRAP} = 1561.538 + (17.562*\mathrm{pH}) - (6.869*\mathrm{Feedflowrate}) + (14.045*\mathrm{TMP}) - - (2.211*\mathrm{pH}*\mathrm{TMP}) - (0.462*\mathrm{pH}^2) + (7.70091\mathrm{E}-003*\mathrm{Feedflowrate}^2) \quad (15)$$

3.4. Effect of pH

In the case of VRF and reversible R, increases in pH generate positive effects on membrane transfer properties throughout the working range, while for Rir, T ORAC, and ABTS, there are points of maximum transfer

and minimum resistance, which indicates the need to find these points to maximize membrane performance. In the present study, unfavorable transfer conditions occur at low pH (Figs. 3-8) because around 4 is the isoelectric point of fish proteins (Belén et al., 2007; Cha et al., 2020), at which these possess zero charge, which affects the resistance to protein elution (Navarro-LisboaBel et al., 2017), given that there is greater precipitation and aggregation between them (Ratnaningsih et al., 2021). In addition, repulsion by the membrane is reduced, which promotes membrane plugging or fouling (Novin and Yunos, 2014).

On the other hand, at pH 10, the highest VRF and permeate flows and lowest hydraulic resistances occurred, while around pH 7 the highest transfers are present. This behavior occurs because, under alkaline conditions, electrostatic repulsion between peptides and membrane can help reduce scale deposition, leading to higher permeate flows (Roslan et al., 2018; Ratnaningsih et al., 2021).

Similar results were obtained by Navarro-Lisboa et al. (2017), who found that flows were higher at a lower ionic strength and higher pH values for quinoa (Chenopodium quinoa Willd.) protein. In the case of whey proteins, permeate flows were higher at high pH (10) but were considerably reduced at pH near the isoelectric point, while 100% protein retention was obtained at pH 4 with protein recovery being 43% at pH 9 (Almécija et al., 2007).

Moreover, Roslan et al. (2018) hydrolyzed byproducts (heads, skeleton, and tail) from tilapia (*Oreochromis niloticus*), which were fractionated on a 5 kDa membrane. It was found that at pH 3 and 5 the lowest permeate flows and lowest transmissions were obtained, while at pH 8 the highest flows and highest peptide transmissions were obtained, this being attributed to electrostatic interactions between the peptides and the membrane.

Other examples include Saidi et al. (2013), who fractionated tuna muscle hydrolysate, finding that the permeate flow was three times higher when going from pH 3 to 8. They concluded that an increase of negative charges on the peptide molecules limits the fouling probably by electrical repulsion between the solute and the membrane surface. There is also a study by Roslan et al. (2018), who achieved the highest peptide transmission at pH 8, yet it was significantly reduced at pH 5. Similar results were obtained in this study, where the highest transmission occurred at medium and high pHs, possibly because these pH variations affect electrostatic peptide-membrane interactions, which affects the transfer of bioactive peptides (Roslan et al., 2021; Saidi et al., 2013).

3.5. Effect of feed flow rate

Feed flow rate is an important factor in the filtration process. This is because working with a low feed flow rate can also lead to decreased permeate flow and can control membrane fouling, since permeate solutes can be swept away and returned to the feed solution (Ogunbiyi et al., 2008; Tomczak and Grita, 2020) as a consequence of the decreased effect of concentration polarization at higher feed flow rates (Almojjly et al., 2019).

This means there is an adequate feed flow rate value (400l/h) and the tangential velocity (3960 m/s) within the working range that favors the response variables. According to the results obtained, the feed flow rate was significant in its linear term for the response variables VRF and T, but Fig. 3 shows that the trend is not very marked regarding the impact of the feed flow rate on the VRF, so the chosen working range does not allow the effect of the increase or decrease of this factor on the response variables to be seen. The same occurs with Figs. 6, 7, and 8, while for Rr and Rir there was no significant effect. Tomczak and Grita (2020) worked with flow values between 200 and 400 L/h and concluded that flows below 400 L/h did not adequately weaken the fouling layer deposited on the membrane surface. They indicated that this maximum flow value corresponded to the transition regime. Therefore, the feed flow rate values in that study are similar to those chosen in this research. Consequently, the choice was adequate.

3.6. TMP effect

Increases in TMP by providing a higher driving force reduces gel layer formation on the membrane surface (Nath et al., 2020), thereby favoring permeate flow, since they increase VRF, mainly at pH close to 10, where proteins are negatively charged and possess higher solubility (Fig. 3). In addition, high TMP values can cause particles to penetrate membrane pores leading to increased irreversible fouling (Im et al., 2019). Therefore, the higher the TMP, the lower the membrane recovery with physical cleaning (Park et al., 2018). The results obtained agree with the above given that the higher the TMP, the higher the irreversible resistance value and the higher the VRF value. In turn, Qi et al. (2022) found that at higher TMP, a more severe fouling of the membrane occurred and a higher permeate flow was achieved, indicating that irreversible fouling caused a possible occurrence of gel layer and pore block. On the other hand, at low TMP, this fouling and concentration polarization can be alleviated, but a lower permeate flow is achieved (Jiang et al., 2018).

Likewise, the formation of these incrustations leads to a higher retention of proteins and high molecular weight molecules, but small peptides (< 3 kDa) continue to pass through the membrane without exceeding 10 bar to avoid reducing the selectivity of the membrane, hence its apparent molecular weight cutoff (Chabeaud et al., 2009), which can improve the concentration of the compounds of interest in the permeate while reducing the process time (Birrenbach et al., 2021). The same occurred in this study; the TMP increase allowed a higher transmission of antioxidant peptides due to a higher penetration through the membrane pores and a higher protein retention, as can be seen in Figs. 5,

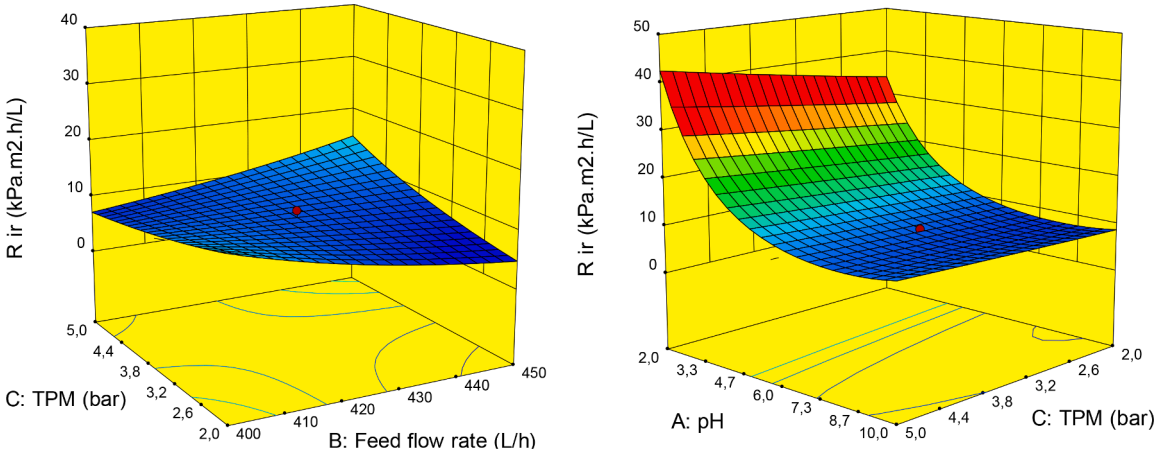

Fig. 5. Response surface for the parameter irreversible resistance as a function of pH, TMP and feed flow rate, predicted by Eq. (12).

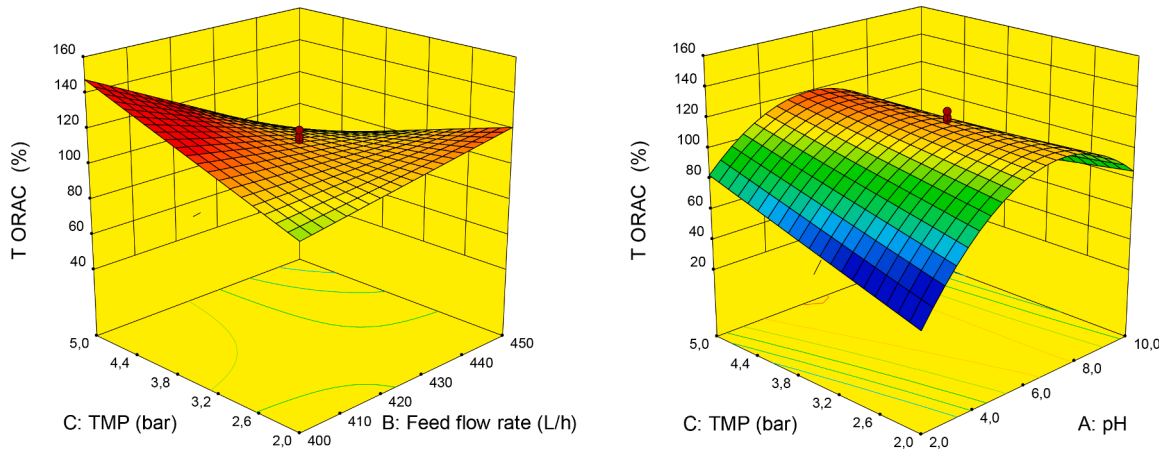

Fig. 6. Response surface for the parameter ORAC transfer as a function of pH, TMP and feed flow rate, predicted by Eq. (13).

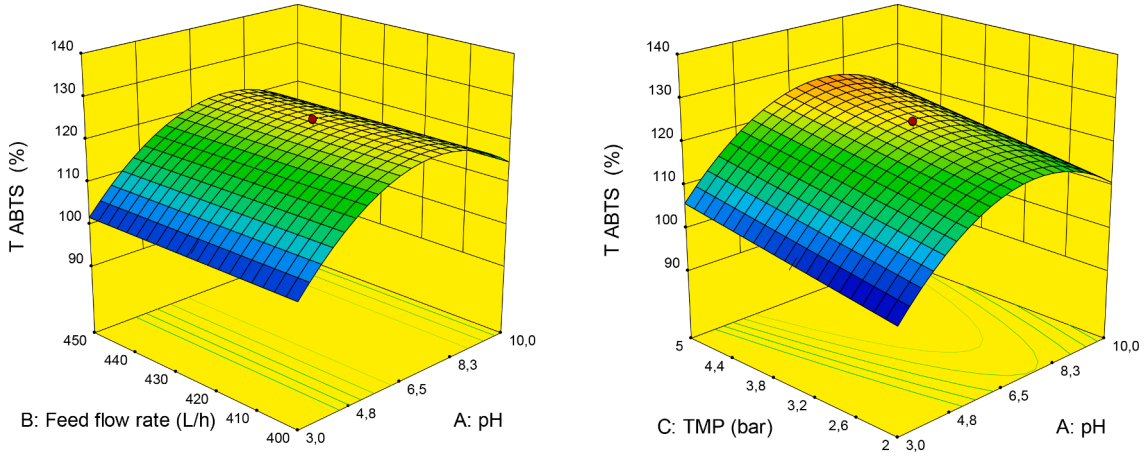

Fig. 7. Response surface for the parameter ABTS transfer as a function of pH, TMP and feed flow rate, predicted by Eq. (14).

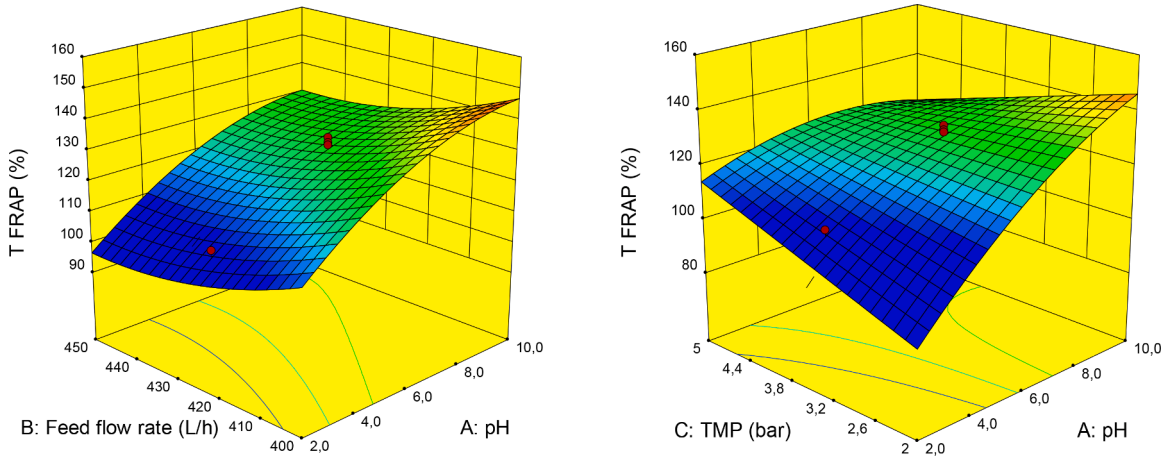

Fig. 8. Response surface for the parameter FRAP transfer as a function of pH, TMP and feed flow rate, predicted by Eq. (15).

6, and 7.

3.7. Model optimization

Equations (10) to (15) were subjected to an optimization process to establish the combination of factors that would maximize peptide transmission (ORAC, ABTS and FRAP) and VRF while minimizing fouling resistances (Rr and Rir), using the Design Expert software (Stat-Ease Inc, USA). The results of the optimal conditions obtained were pH 8.39, TMP 5 bar, and feed flow rate 400 L/h. Table 5 shows the values of the response variables, both experimental and predicted, obtained under these conditions. It is observed that the experimental values are adjusted to the predicted ones, which displays the effectiveness of the response surface methodology as an optimization method. Based on the relative

Table 5
Predicted and experimental values obtained under the optimal conditions of the central composite factorial design.

Response	Predicted	Experimental	Relative error (%)
T ORAC (%)	130.994	136.310 ± 3.075	4.058
T ABTS (%)	125.55	126.374 ± 0.830	0.656
T FRAP (%)	138.09	131.858 ± 1.270	4.513
VRF	1.585	1.612 ± 1.310	1.689
Rr (kPa m^2 h/L)	4.560	4.385 ± 0.354	4.671
Rir (kPa m^2 h/L)	6.756	6.205 ± 0.021	8.159

Table 6
Antioxidant activity values of the complete hydrolysate and fractions < 3 kDa and > 3 kDa.

Sample	Time (h)	ORAC (μ-eqmol-trolox/g protein)	ABTS (μ-eqmol-trolox /g protein)	FRAP (μ-eqmol-trolox /g protein)
Hydrolysate		527.284^{a} ± 11.120	1657.523^{a} ± 19.387	116.058^{a} ± 2.105
Permeate <3kDa	2	762.517^{b} ± 17.568	2070.781^{b} ± 60.403	149.524^{b} ± 3.624
Retentate >3kDa	2	351.311^{c} ± 0.474	1507.295^{c} ± 1.286	112.885^{c} ± 2.074

Table 7
Mass balance in terms of protein.

Parameter	Feed solution	Permeate	Retentate
Volume (L)	2442 ± 0,006	0,938 ± 0,025	1452 ± 0,008
Protein (g/L)	9669 ± 0,006	5292 ± 0,083	12,936 ± 0,104
Grams of protein	23,624 ± 0,078	4966 ± 0,912	18,785 ± 1608
Relative error (%)	−0,538		

Table 8
Amino acid composition of red tilapia (*Oreochromis spp*.) viscera hydrolysate and fractions < 3 kDa and > 3 kDa.

Amino acid	Complete hydrolysate (mg/g)	Fraction < 3 kDa (mg/g)	Fraction >3 kDa (mg/g)
ASP	5.520	3.752	2.342
GLU	9.396	9.301	5.474
ASN	1.002	1.387	N/A
SER	6.290	7.964	3.651
HIS	10.481	18.648	9.075
GLY	26.080	34.065	14.345
THR	4.608	8.194	3.265
ARG	8.104	11.706	3.942
ALA	7.155	6.414	2.756
TYR	5.932	35.214	2.446
CYS	6.177	13.769	3.170
VAL	7.807	11.168	4.494
MET	3.451	5.861	2.444
PHE	0.837	0.218	0.135
ILE	4.088	5.790	2.247
LEU	11.023	14.038	5.798
LYS	12.632	13.822	6.217
HYP	N/A	N/A	N/A
PRO	N/A	N/A	N/A

error values, the models can adequately predict the behavior of the response variables as a function of the factors.

The values of antioxidant activities of both the unfractionated hydrolysate and the < 3 kDa and >3 kDa fractions are shown in Table 6, where with these results, the increased antioxidant capacity in the permeate is evident. This is relevant because it shows that the most potent peptides are found in the lower molecular weight fractions, since they have higher biological activity (Pezeshk et al., 2019). This is the case for other hydrolyzed fish byproducts (*herring milt*), where they determined that the initial hydrolysate had an ORAC activity of 218.32 (μmol ET/g) and the fractionated hydrolysate 687.18 (μmol ET/g) (Durand et al., 2019). Also, Pezeshk et al. (2019) found the highest activity (66% at 2 mg/ml) in the <3 kDa fraction by ABTS radical scavenging activity.

The retention coefficients of antioxidant peptides in the permeate calculated from Table 6 results, had values of −24.932%, −44.612% and −28.836% for ABTS, FRAP and ORAC activity, respectively. These negative values mean that the antioxidant peptides are being concentrated in the <3 kDa fraction, which is the main objective of this work.

In order to calculate the amount of mass (in terms of protein) remaining at the end of the process, a mas balance was carried out, including the initial values for the hydrolysate and the final values for the retained and the permeate. It was found that there was a higher protein retention in the retained (Table 7), while, there was higher antioxidant peptides content in the <three kDa fraction (Table 6), obtaining an enriched permeate in interest peptides.

3.8. Amino acid analysis

Membrane fractionation allowed a higher amount of free amino acids and peptides in the permeate (< 3 kDa) to be concentrated, as can be seen in Table 8, which is the fraction of interest for this study, compared to the retaining (> 3 kDa) and the initial hydrolysate.

The amino acid composition of the different samples had mostly Gly, where peptides containing this amino acid have a strong antioxidant power (Yang et al., 2020). Likewise, Tyr, His, Lys, Arg, Ala, Val, and Leu, which predominate over the other amino acids, foster antioxidant peptide activity (Pezeshk et al., 2019; Nikoo et al., 2019). In addition, hydrophobic and aromatic amino acid residues are related to this kind of activity. Therefore, these properties and the amino acids present influence the increase of the antioxidant activity of the < 3 kDa fraction of red tilapia (*Oreochromis spp*.) viscera hydrolysate, where one of the mechanisms of action may be stabilization of active oxygen through direct electron transfer (Pezeshk et al., 2019).

4. Conclusion

Antioxidant bioactive peptides from viscera hydrolysates are highly relevant due to their biological properties; therefore, a need for an adequate separation and obtaining for their subsequent use was evidenced. By using cross-flow filtration with ceramic membranes, an efficient process can be achieved. Of the variables evaluated, the effect of pH on the RVF and both irreversible and reversible resistances was evidenced, given that there was greater fouling of the membrane and low permeate volumes at acid pH.

It was also found that at the upper limits used in the experimental design, TMP did not decrease the process yield and bioactivity of peptides in the permeate. Moreover, in the selected feed flow rate range, there was no marked effect of TMP on the filtration process. Regarding the bioactive peptides, the < 3 kDa fraction expressed a better antioxidant property in respect to the initial hydrolysate; thus, filtration with ceramic membranes is recommended to obtain a potentially nutraceutical product.

Declaration of competing interest

The authors declare that they have no known competing financial interests or personal relationships that could have appeared to influence the work reported in this paper.

Funding

This work was supported by the Administrative Department of Science, Technology and Innovation (Minciencias) through its call for

national doctorates.

References

Abdullayev, A., Bekheet, M.F., Hanaor, D.A., Gurlo, A., 2019. Materials and applications for low-cost ceramic membranes. Membranes 9 (9), 105. https://doi.org/10.3390/membranes9090105.

Almécija, M.C., Ibáñez, R., Guadix, A., Guadix, E.M., 2007. Effect of pH on the fractionation of whey proteins with a ceramic ultrafiltration membrane. J. Membr. Sci. 288 (1-2), 28–35. https://doi.org/10.1016/j.memsci.2006.10.021.

Almojjly, A., Johnson, D., Hilal, N., 2019. Investigations of the effect of pore size of ceramic membranes on the pilot-scale removal of oil from oil-water emulsion. J. Water Process Eng. 31, 100868 https://doi.org/10.1016/j.jwpe.2019.100868.

AOAC (Association of Official Analytical Chemists). Official Methods of Analysis of AOAC international (14th Ed.). Washington, D.C., U.S.A. 1984.

Aspevik, T., Thoresen, L., Steinsholm, S., Carlehög, M., Kousoulaki, K., 2021. Sensory and chemical properties of protein hydrolysates based on mackerel (Scomber scombrus) and salmon (Salmo salar) side stream materials. J. Aquat. Food Prod. Technol. 30 (2), 176–187. https://doi.org/10.1080/10498850.2020.1868644.

Belén Camacho R, D.R., Moreno Álvarez, M.J., García, D., Medina, C., Sidorovas, A, 2007. Caracterización de un hidrolizado proteico enzimático obtenido del pez caribe colorado (*Pygocentrus cariba Humboldt, 1821*). Interciencia 32 (3), 188–194. http://ve.scielo.org/scielo.php?pid=S0378-18442007000300011&script=sci_abstract.

Benítez, R., Ibarz, A., Pagan, J., 2008. Hidrolizados de proteína: procesos y aplicaciones. Acta bioquímica clínica latinoamericana 42 (2), 227–236. http://www.scielo.org.ar/scielo.php?pid=S0325-29572008000200008&script=sci_arttext&tlng=pt.

Birrenbach, O., Faust, F., Ebrahimi, M., Fan, R., Czermak, P., 2021. Recovery and purification of protein aggregates from cell lysates using ceramic membranes: fouling analysis and modeling of ultrafiltration. Front. Chem. Eng. 3 (9) https://doi.org/10.3389/fceng.2021.656345.

Castro-Muñoz, R., Barragán-Huerta, B.E., Fíla, V., Denis, P.C., Ruby-Figueroa, R., 2018. Current role of membrane technology: from the treatment of agro-industrial by-products up to the valorization of valuable compounds. Waste Biomass Valorization 9 (4), 513–529. https://doi.org/10.1007/s12649-017-0003-1.

Cha, J.W., Yoon, I.S., Lee, G.W., Kang, S.I., Park, S.Y., Kim, J.S., Heu, M.S., 2020. Food functionalities and bioactivities of protein isolates recovered from skipjack tuna roe by isoelectric solubilization and precipitation. Food. Sci. Nutr. 8 (4), 1874–1887. https://doi.org/10.1002/fsn3.1470.

Chabeaud, A., Vandanjon, L., Bourseau, P., Jaouen, P., Chaplain-Derouiniot, M., Guérard, F., 2009. Performances of ultrafiltration membranes for fractionating a fish protein hydrolysate: application to the refining of bioactive peptidic fractions. Sep. Purif. Technol. 66 (3), 463–471. https://doi.org/10.1016/j.seppur.2009.02.012.

Chi, C.F., Hu, F.Y., Wang, B., Ren, X.J., Deng, S.G., Wu, C.W., 2015. Purification and characterization of three antioxidant peptides from protein hydrolyzate of croceine croaker (*Pseudosciaena crocea*) muscle. Food. Chem. 168, 662–667. https://doi.org/10.1016/j.foodchem.2014.07.117.

Cigić, I.K., Vodošek, T.V., Košmerl, T., Strlič, M., 2008. Amino acid quantification in the presence of sugars using HPLC and pre-column derivatization with 3-MPA/OPA and FMOC-Cl. Acta Chim. Slov. 55 (3). http://acta-arhiv.chem-soc.si/55/55-3-660.pdf.

Durand, R., Fraboulet, E., Marette, A., Bazinet, L., 2019. Simultaneous double cationic and anionic molecule separation from herring milt hydrolysate and impact on resulting fraction bioactivities. Sep. Purif. Technol. 210, 431–441. https://doi.org/10.1016/j.seppur.2018.08.017.

Espejo-Carpio, F.J., Pérez-Gálvez, R., Almécija, M.D.C., Guadix, A., Guadix, E.M., 2015. Increasing the angiotensin converting enzyme inhibitory activity of goat milk hydrolysates by cross-flow filtration through ceramic membranes. Desalin. Water Treat. 56 (13), 3544–3553. https://doi.org/10.1080/19443994.2014.985729.

FAO, 2020. El Estado Mundial De La Pesca y La Acuicultura 2020. La sostenibilidad en acción, Roma.

Gianfranceschi, G.L., Gianfranceschi, G., Quassinti, L., Bramucci, M., 2018. Biochemical requirements of bioactive peptides for nutraceutical efficacy. J. Funct. Foods 47, 252–263. https://doi.org/10.1016/j.jff.2018.05.034.

Gómez Sampedro, L.J., Figueroa Moreno, O.A., Zapata Montoya, J.E., 2013. Actividad antioxidante de hidrolizados enzimáticos de plasma bovino obtenidos por efecto de alcalasa® 2.4 L. Inf. Tecnol. 24 (1), 33–42. https://doi.org/10.4067/S0718-07642013000100005.

Gómez, L.J., Gómez, N.A., Pereañez, J.A., Zapata, J.E., 2019. Lipids as competitive inhibitors of subtilisin carlsberg in the enzymatic hydrolysis of proteins in red tilapia (*oreochromis sp.)* viscera: insights from kinetic models and a molecular docking study. Braz. J. Chem. Eng. 36 (2), 647–655. https://doi.org/10.1590/0104-6632.20190362s20180346.

Halim, N.R.A., Yusof, H.M., Sarbon, N.M., 2016. Functional and bioactive properties of fish protein hydolysates and peptides: a comprehensive review. Trends Food Sci. Technol. 51, 24–33. https://doi.org/10.1016/j.tifs.2016.02.007.

Hanachi, A., Bianchi, A., Kahn, C.J., Velot, E., Arab-Tehrany, E., Cakir-Kiefer, C., Linder, M., 2022. Encapsulation of salmon peptides in marine liposomes: physico-chemical properties, antiradical activities and biocompatibility assays. Mar. Drugs. 20 (4), 249. https://doi.org/10.3390/md20040249.

Im, D., Nakada, N., Kato, Y., Aoki, M., Tanaka, H., 2019. Pretreatment of ceramic membrane microfiltration in wastewater reuse: a comparison between ozonation and coagulation. J. Environ. Manage. 251, 109555 https://doi.org/10.1016/j.jenvman.2019.109555.

Jiang, S., Zhang, Y., Zhao, F., Yu, Z., Zhou, X., Chu, H., 2018. Impact of transmembrane pressure (TMP) on membrane fouling in microalgae harvesting with a uniform shearing vibration membrane system. Algal Res. 35, 613–623. https://doi.org/10.1016/j.algal.2018.10.003.

Li, W., Ling, G., Lei, F., Li, N., Peng, W., Li, K., Zhang, Y., 2018. Ceramic membrane fouling and cleaning during ultrafiltration of limed sugarcane juice. Sep. Purif. Technol. 190, 9–24. https://doi.org/10.1016/j.seppur.2017.08.046.

Liu, Y., Li, X., Chen, Z., Yu, J., Wang, F., Wang, J., 2014. Characterization of structural and functional properties of fish protein hydrolysates from surimi processing by-products. Food Chem. 151, 459–465. https://doi.org/10.1016/j.foodchem.2013.11.089.

Liu, Y.C., Yang, Y.J., Chen, M.S., Wang, L., Lu, S.G., Liu, S.H., Shan, Y.M., 2018. Adjustment of prescription by ORAC assay to enhance the effect of medicinal liqueur. J. Food Eng. Technol. 7 (1), 36–42. https://doi.org/10.32732/jfet.http://xpublication.com/index.php/jfet/article/view/179/109.

Liu, W.Y., Fang, L., Feng, X.W., Li, G.M., Gu, R.Z., 2020. In vitro antioxidant and angiotensin I-converting enzyme inhibitory properties of peptides derived from corn gluten meal. Eur. Food Res. Technol. 246 (10), 2017–2027. https://doi.org/10.1007/s00217-020-03552-6.

Liu, W.Y., Zhang, J.T., Miyakawa, T., Li, G.M., Gu, R.Z., Tanokura, M., 2021. Antioxidant properties and inhibition of angiotensin-converting enzyme by highly active peptides from wheat gluten. Sci. Rep. 11 (1), 1–13. https://doi.org/10.1038/s41598-021-84820-7.

Luján-Facundo, M.J., Mendoza-Roca, J.A., Cuartas-Uribe, B., Álvarez-Blanco, S., 2017. Membrane fouling in whey processing and subsequent cleaning with ultrasounds for a more sustainable process. J. Cleaner Prod. 143, 804–813. https://doi.org/10.1016/j.jclepro.2016.12.043.

Lyu, Z., Ng, T.C.A., Gu, Q., Sun, Q., He, Z., Zhang, L., Wang, J., 2019. Nanowires versus nanosheets–effects of NiCo2O4 nanostructures on ceramic membrane permeability and fouling potential. Sep. Purif. Technol. 215, 644–651. https://doi.org/10.1016/j.seppur.2019.01.060.

Martínez-Medina, G.A., Prado-Barragán, A., Martínez-Hernández, J.L., Ruíz, H.A., Rodríguez, R.M., Contreras-Esquivel, J.C., Aguilar, C.N., 2019. Péptidos Biofuncionales: bioactividad, producción y aplicaciones. Rev. Cient. Univ. Autón Coah. 13 (22). http://www.biochemtech.uadec.mx/wp-content/uploads/2022/01/PeptidosBiofuncionales.pdf.

Merino, M.C., Bonilla, S.P., Bages, F., 2013. Diagnóstico Del Estado De La Acuicultura En Colombia. Plan Nacional De Desarrollo de La Acuicultura Sostenible En Colombia AUNAP-FAO. Ministerio de Agricultura y Desarrollo Rural, Bogotá, Colombia.

Montero-Barrantes, M., 2021. Hidrolizados proteícos a partir de subproductos de la industria pesquera: obtención y funcionalidad. Agron. Mesoam. 32 (2), 681–699. https://doi.org/10.15517/AM.V32I2.41437.

Nalinanon, S., Benjakul, S., Kishimura, H., Shahidi, F., 2011. Functionalities and antioxidant properties of protein hydrolysates from the muscle of ornate threadfin bream treated with pepsin from skipjack tuna. Food Chem. 124 (4), 1354–1362. https://doi.org/10.1016/j.foodchem.2010.07.089.

Nath, K., Dave, H.K., Patel, T.M., 2018. Revisiting the recent applications of nanofiltration in food processing industries: progress and prognosis. Trends Food Sci. Technol. 73, 12–24. https://doi.org/10.1016/j.tifs.2018.01.001.

Nath, A., Eren, B.A., Csighy, A., Pásztorné-Huszár, K., Kiskó, G., Abrankó, L., Vatai, G., 2020. Production of liquid milk protein concentrate with antioxidant capacity, angiotensin converting enzyme inhibitory activity, antibacterial activity, and hypoallergenic property by membrane filtration and enzymatic modification of proteins. Processes 8 (7), 871. https://doi.org/10.3390/pr8070871.

Navarro-Lisboa, R., Herrera, C., Zúñiga, R.N., Enrione, J., Guzmán, F., Matiacevich, S., Astudillo-Castro, C., 2017. Quinoa proteins (*Chenopodium quinoa Willd.*) fractionated by ultrafiltration using ceramic membranes: the role of pH on physicochemical and conformational properties. Food Bioprod. Process. 102, 20–30. https://doi.org/10.1016/j.fbp.2016.11.005.

Nikoo, M., Benjakul, S., Yasemi, M., Gavlighi, H.A., Xu, X., 2019. Hydrolysates from rainbow trout (*Oncorhynchus mykiss*) processing by-product with different pretreatments: antioxidant activity and their effect on lipid and protein oxidation of raw fish emulsion. LWT 108, 120–128. https://doi.org/10.1016/j.lwt.2019.03.049.

Novin, D., Yunos, K.M., 2014. Effect of operating parameters on performance of ultrafiltration (UF) to fractionate catfish protein hydrolysate. J. Teknol. 70 (2), 11–14. https://doi.org/10.11113/jt.v70.3427.

Ogunbiyi, O.O., Miles, N.J., Hilal, N., 2008. The effects of performance and cleaning cycles of new tubular ceramic microfiltration membrane fouled with a model yeast suspension. Desalination 220 (1–3), 273–289. https://doi.org/10.1016/j.desal.2007.01.034.

Park, S., Kang, J.S., Lee, J.J., Vo, T.K.Q., Kim, H.S., 2018. Application of physical and chemical enhanced backwashing to reduce membrane fouling in the water treatment process using ceramic membranes. Membranes 8 (4), 110. https://doi.org/10.3390/membranes8040110.

Pezeshk, S., Ojagh, S.M., Rezaei, M., Shabanpour, B., 2019. Fractionation of protein hydrolysates of fish waste using membrane ultrafiltration: investigation of antibacterial and antioxidant activities. Probiotics Antimicrob. Proteins. 11 (3), 1015–1022. https://doi.org/10.1007/s12602-018-9483-y.

Qi, T., Yang, D., Chen, X., Qiu, M., Fan, Y., 2022. Rapid removal of lactose for low-lactose milk by ceramic membranes. Sep. Purif. Technol., 120601 https://doi.org/10.1016/j.seppur.2022.120601.

Ratnaningsih, E., Reynard, R., Khoiruddin, K., Wenten, I.G., Boopathy, R., 2021. Recent advancements of UF-based separation for selective enrichment of proteins and bioactive peptides—a review. Appl. Sci. 11 (3), 1078. https://doi.org/10.3390/app11031078.

Roslan, J., Kamal, S.M.M., Yunos, K.F.M., Abdullah, N., 2017. Assessment on multilayer ultrafiltration membrane for fractionation of tilapia by-product protein hydrolysate

with angiotensin I-converting enzyme (ACE) inhibitory activity. Sep. Purif. Technol. 173, 250–257.
Roslan, J., Kamal, S.M.M., Yunos, K.F.M., Abdullah, N., 2018. Evaluation on performance of dead-end ultrafiltration membrane in fractionating tilapia by-product protein hydrolysate. Sep. Purif. Technol. 195, 21–29. https://doi.org/10.1016/j.seppur.2017.11.020.
Roslan, J., Mustapa Kamal, S.M., Abdullah, N., 2021. Fractionation of tilapia by-product protein hydrolysate using multilayer configuration of ultrafiltration membrane. Processes 9 (3), 446. https://doi.org/10.3390/pr9030446.
Saidi, S., Deratani, A., Amar, R.B., Belleville, M.P., 2013. Fractionation of a tuna dark muscle hydrolysate by a two-step membrane process. Sep. Purif. Technol. 108, 28–36. https://doi.org/10.1016/j.seppur.2013.01.048.
Saidi, S., Deratani, A., Belleville, M.P., Amar, R.B., 2014. Production and fractionation of tuna by-product protein hydrolysate by ultrafiltration and nanofiltration: impact on interesting peptides fractions and nutritional properties. Food Res. Int. 65, 453–461. https://doi.org/10.1016/j.foodres.2014.04.026.
Sánchez, A., Vázquez, A., 2017. Bioactive peptides: a review. Food Qual. Saf. 1 (1), 29–46. https://doi.org/10.1093/fqsafe/fyx006.
Sepúlveda, C.T., Zapata, J.E., 2020. Effects of enzymatic hydrolysis conditions on the antioxidant activity of red Tilapia (*Oreochromis spp.*) viscera hydrolysates. Curr. Pharm. Biotechnol. 21 (12), 1249–1258. https://doi.org/10.2174/1389201021666200506072526.
Sila, A., Bougatef, A., 2016. Antioxidant peptides from marine by-products: isolation, identification and application in food systems. A review. J. Funct. Foods. 21, 10–26. https://doi.org/10.1016/j.jff.2015.11.007.
Solís, C.A., Vélez, C.A., Ramírez-Navas, J.S., 2017. Tecnología de membranas: Ultrafiltración. Entre Cienc. Ing. 11 (22), 26–36. https://doi.org/10.31908/19098367.3546.
Tomczak, W., Gryta, M., 2020. Clarification of 1,3-propanediol fermentation broths by using a ceramic fine UF membrane. Membranes 10 (11), 319. https://doi.org/10.3390/membranes10110319.
Tonon, R.V., dos Santos, B.A., Couto, C.C., Mellinger-Silva, C., Brígida, A.I.S., Cabral, L. M., 2016. Coupling of ultrafiltration and enzymatic hydrolysis aiming at valorizing shrimp wastewater. Food Chem. 198, 20–27. https://doi.org/10.1016/j.foodchem.2015.11.094.
Urbanowska, A., Kabsch-Korbutowicz, M., 2019. Nanofiltration as an effective method of NaOH recovery from regenerative solutions. Arch. Environ. Prot. 45 (2) https://doi.org/10.24425/aep.2019.127978.
Valcárcel, J., Sanz, N., Vázquez, J.A., 2020. Optimization of the Enzymatic Protein Hydrolysis of By-Products from Seabream (*Sparus aurata*) and Seabass (*Dicentrarchus labrax*). Chem. Funct. Charact. Foods 9 (10), 1503. https://doi.org/10.3390/foods9101503.
Vasconcelos, J.B., de Vasconcelos, E.R., Urrea-Victoria, V., Bezerra, P.S., Reis, T.N., Cocentino, A.L., Fujii, M.T., 2019. Antioxidant activity of three seaweeds from tropical reefs of Brazil: potential sources for bioprospecting. J. Appl. Phycol. 31 (2), 835–846. https://doi.org/10.1007/s10811-018-1556-5.
Villamil, O., Váquiro, H., Solanilla, F., 2017. Fish viscera protein hydrolysates: production, potential applications and functional and bioactive properties. Food Chem. 224, 160–171. https://doi.org/10.1016/j.foodchem.2016.12.057.
Wen-Qiong, W., Yun-Chao, W., Xiao-Feng, Z., Rui-Xia, G., Mao-Lin, L., 2019. Whey protein membrane processing methods and membrane fouling mechanism analysis. Food Chem. 289, 468–481. https://doi.org/10.1016/j.foodchem.2019.03.086.
Yang, Q., Cai, X., Yan, A., Tian, Y., Du, M., Wang, S., 2020. A specific antioxidant peptide: its properties in controlling oxidation and possible action mechanism. Food Chem. 327, 126984 https://doi.org/10.1016/j.foodchem.2020.126984.
Zheng, P., Hao, G., Weng, W., Ren, H., 2019. Antioxidant activities of hydrolysates from abalone viscera using subcritical water-assisted enzymatic hydrolysis. Food Bioprocess Technol. 12 (6), 910–918. https://doi.org/10.1007/s11947-019-02270-6.